Long term corrosion investigation of cold rolled high nitrogen steels in simulated body fluid

Mohd Talha[*1] and O.P. Sinha[2]

[1]Department of Chemistry, Faculty of Science, P.D. Degree College, Bhorugram, Rajgarh-331023, Churu, Rajasthan, India

[2]Centre of Advanced Study, Department of Metallurgical Engineering, Indian Institute of Technology (Banaras Hindu University), Varanasi-221005, Uttar Pradesh, India

Abstract

The corrosion behavior of cold rolled and annealed (solution treated from 1050 °C) Ni-free high nitrogen austenitic stainless steels (HNSs) was assessed in simulated body fluid (SBF) using weight loss (long term) method. Surface analysis of the films formed and composition of species on these steels exposed to SBF was done using X-ray photoelectron spectroscopy (XPS). It was detected that increase in nitrogen content significantly increased the corrosion resistance i.e. decreased weight loss in solution annealed (0% cold worked) condition. The cold working had noteworthy impact on the corrosion resistant properties. The weight loss and corrosion rates decreased with increasing degree of cold working and nitrogen content in the alloy. The XPS results indicated that the main elements in the passive oxide layer are Cr, Fe, Mo and Mn. Cr-

1

oxide (ox) :Cr-hydroxide(hy) ratio and Fe-oxide (ox) : Fe-hydroxide (hy) ratio were observed higher in case of rolled material than annealed material indicating that the passive films on rolled materials are more protective which correspond to slow dissolution rate and improve its corrosion resistance. X-ray diffraction profiles of annealed as well as deformed alloys were revealed and no evidence of formation of martensite or any other secondary phases was observed.

Keywords: Corrosion, HNS, Cold working, SBF, XPS

*Corresponding author: [1]mohd.talha.rs.met@itbhu.ac.in; Phone: +91-9997993459, Fax: +91-542-2369478

1. Introduction

Among various metallic materials used for orthopedic implants, austenitic stainless steels(e.g. 316L) is one of the most extensively used for internal fixation devices like fracture plates, screws, hip nail and artificial joints because of their good mechanical properties, corrosion resistance, easy processing, acceptable biocompatibility and very low cost as compared with those of other metallic implant materials [1-3]. These conventional stainless steels (SSs) contain nickel (12.0-15.0%) and release of nickel ions from SS due to corrosion results negative reactions in the body at normal physiological conditions [4, 5]. Therefore, the austenitic stabilizing property of

2

nitrogen allows the nickel content in steel to be reduced practically to zero, offering further advantages such as lower production costs, higher strength, additional corrosion resistance and also excellent biocompatibility [6]. Up to now, all in-vivo and in-vitro studies strongly suggested that Ni-free high nitrogen austenitic stainless steels (HNSs) would be a class of favorable biomaterials for medical applications [6, 7, 8]. Corrosion of SSs in human body can bound their application in bio-systems. The corrosion resistance property of SS is affected by metallurgical parameters [9, 10] like, cold working (c. w.) alloy composition, inclusions, heat treatment, grain size, sensitization, and secondary precipitates. SSs are subjected to different stages of cold working during the final manufacturing stages of components. Many investigations have been carried out in the past on effect of cold working on corrosion resistance of SSs [11-13]. Beddoes and Bucci studied weight loss of 316L during 72 hour immersion tests at 22 and 37˚C in of 6% ferric chloride solution and stated average weight loss as a function of surface roughness [14]. Increasing surface roughness caused in faster weight loss at 22˚C but weight loss was independent of the surface roughness at 37 ˚C. Shima Karimi et al.[15] studied the long term weight loss of AISI 316L, the Co-28Cr-6Mo and Ti-6Al-4V alloys in PBS with various bovine serum albumin (BSA) concentrations. They detected that all the samples lost weight up to 14 weeks and then started to gain weight.

The aspect of cold working has not been yet associated clearly to the influence on the corrosion resistance of HNSs in simulated body fluid (SBF) especially for long term

applications. In the present work, an effort was made to study the effect of cold working on the long term corrosion resistance of HNSs with different nitrogen contents in SBF. The method used in this study was static immersion test (weight loss method). To analyze the effect of carbon with nitrogen on weight loss, one alloy which contains high nitrogen (0.34 wt. %) as well as carbon (0.48 wt. %) was also selected for the present study. XPS was also used to detect the chemical composition of the passive film formed on surface of SSs after 1 h of immersion in SBF. To identify the phases present after cold working, X-ray diffraction (XRD) profiles of the annealed and cold worked (c.w.) samples were carried out. The results obtained were compared with conventionally used nickel grade; AISI 316LVM.

2. Materials and Methods

Three HNSs (316MnN$_1$, 316MnN$_2$ and 316MnN$_3$) with different nitrogen contents were prepared in the form of ingots respectively by melting Armco iron and ferro alloys in appropriate proportions to meet the aimed composition of alloy in an induction   furnace.   These ingots were solutionized at 1050-1070 ℃ to avoid segregation. Then samples as slices of 80 $\times$ 20 $\times$ 6 mm were cut from ingot, hot-rolled at 1050 ℃ to reduce thickness by 50-80%, the solution treated at 1050-1070 ℃ for 15 min, and then water quenched respectively. 316LVM SS was obtained from Mishra Dhatu Nigam Ltd. (MIDHANI), Hyderabad, India. This steel was received in hot

rolled & annealed condition and used for study in similar condition. All the annealed specimens of 80 × 12 × 2 mm were cut and cold rolled to 10% and 20% reductions in thickness values. The chemical compositions of all four austenitic SSs are shown in Table 1.

Table 1

Composition of stainless steels (wt. %)

Sample	C	Cr	Mn	Ni	Si	Mo	S	P	N	Fe
316LVM	0.02	17.24	1.68	14.42	0.24	2.83	0.004	0.007	0.07	Bal.
316MnN$_1$	0.48	19.32	12.77	0.05	0.26	3.32	0.006	0.009	0.34	Bal.
316MnN$_2$	0.08	19.11	11.85	0.08	0.25	3.02	0.004	0.010	0.43	Bal.
316MnN$_3$	0.017	18.28	11.92	0.04	0.07	3.24	0.003	0.008	0.52	Bal.

For the immersion tests, specimens of 20 x 10 mm with their original thickness were cut from annealed and rolled strips with a 1.5 mm-diameter hole at one end, abraded successively with emery papers of 600, 800, 1000 and 1200 grades, washed with deionized water followed by acetone and dried. Each coupon was weighed on a Mettler Toledo JB1603 balance with a precision of 0.001 mg just before immersion in the solution. After removing the samples from the test solutions, they were rinsed with deionized water and ethanol, and dried in air, and then the final weight loss was measured using the same scales. The procedure of using beakers for immersion test was followed by ASTM standard D5245-92 [16]. Each coupon of SS was hung by fluorocarbon plastic strings in a separate beaker and fully

submerged vertically in 120 ml of solution. The SBF used for the immersion test was Ringer's physiological solution of pH value 7.4±0.2 prepared in deionized water (Table 2) [17]. All the beakers, covered with perforated rubber cork, were placed inside a thermostat for 12 to 24 weeks at 37 °C with an accuracy of 0.2 °C which is equivalent to human body temperature [18]. The water levels in the beakers were checked every three days and deionized water was added if solution levels decreased. XPS (AMICUS, Kratos Analytical, Shimadzu, U.K.) was used to detect the chemical composition of the passive film formed on working electrode after 1 h of immersion in SBF solution. The Mg Kα line was used as the X-ray source. A survey spectrum together with high resolution regions of Fe 2p, Cr 2p, Mo 3d, Mn 2p, O 1s, N 1s and C 1s were recorded. The C 1s peak was assumed to be at 285.4 eV and was used as an internal standard to determine the binding energy of other photoelectron peaks. Linear background subtraction was made to obtain the XPS signal intensity. XRD analysis of samples was carried out using a Rigaku Miniflex II X-ray diffractometer. The Cu Kα line was used as the X-ray source.

Table 2

Composition of Ringer's physiological solution (g/L)[17]

Components	NaCl	KCl	$CaCl_2$	$NaHCO_3$
Wt. %	9.0	0.40	0.25	0.20

3. Results and discussion

3.1. Weight loss

The weight loss of different SSs up to the 24 week immersion with time is presented in Fig. 1. The points refer to the average weight loss of six measurements and an error bar is the standard deviation.
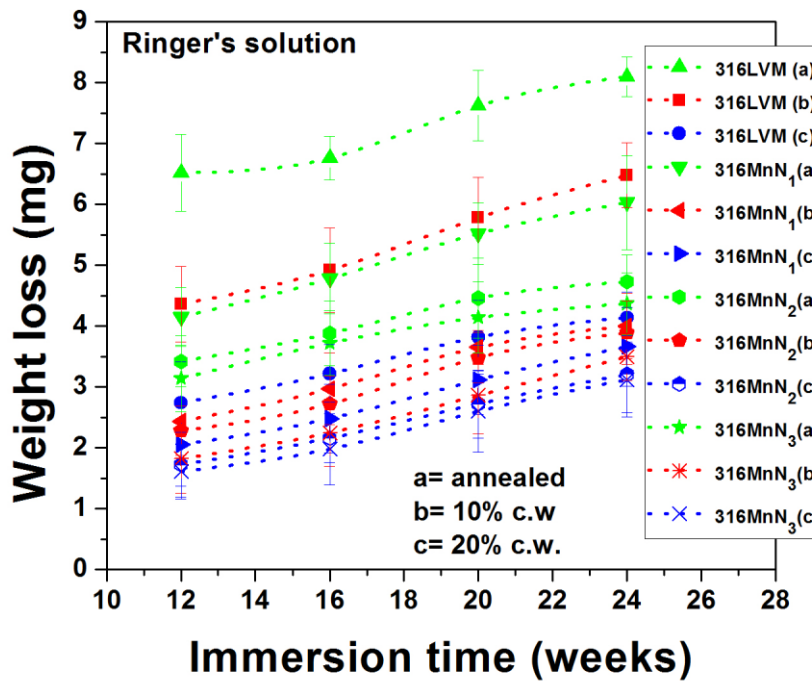

Fig. 1: Weight loss versus immersion time at 37 °C for tested SSs in Ringer's solution.

It can be seen from the figure that weight loss increases with time. The surfaces of all the samples were examined using both optical and scanning electron microscope (FEI Quanta 200FEG). No sign of localized corrosion was detected on any specimens.

Therefore, the weight loss data was used to calculate the corrosion rates by following equation (ASTM G31-72) [19].

Corrosion rate (μm/year) $= \dfrac{K \times W}{A \times T \times D}$

where K is a constant (8.76×10^4), T is time of exposure (in hours), A is area of immersed specimen (in cm^2), W is mass loss (in mg) and D is density of alloy (in g/cm^3). Fig. 2 shows the variation of the corrosion rates, as a function of cold working and nitrogen content in the alloy after 24 weeks of immersion in SBF. It was observed that the weight loss and corrosion rate decreased with increasing nitrogen content and degree of cold working.
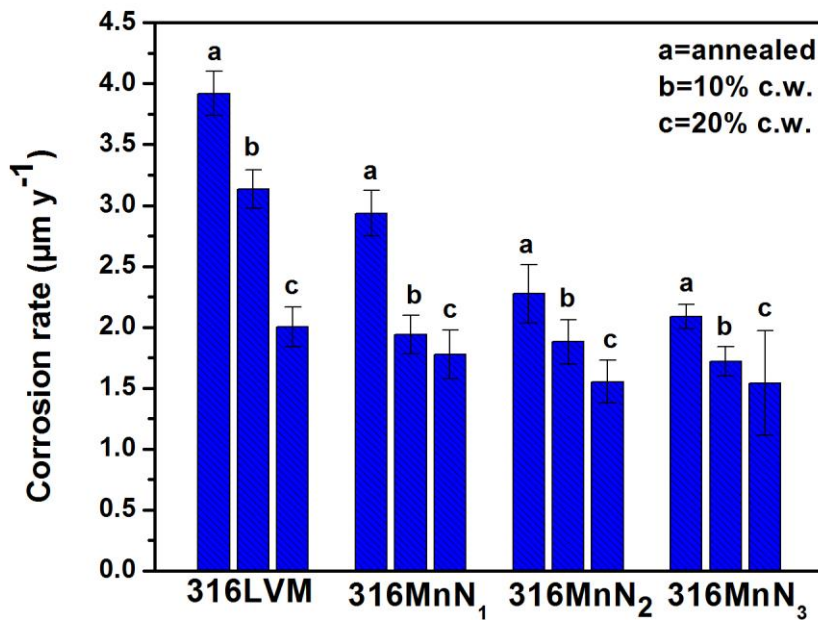

Fig. 2: Variation of the corrosion rates, as a function of cold working and nitrogen content after 24 weeks of immersion in SBF

3.2. X-Ray Photoelectron Spectroscopy (XPS) analysis

Results of surface analysis of passive films by XPS of annealed and 20% cold worked 316MnN$_3$ SS are shown in Fig. 3. Iron, chromium, molybdenum, oxygen, nitrogen and manganese were the species detected in the survey scan, whereas nickel was absent in both the samples.
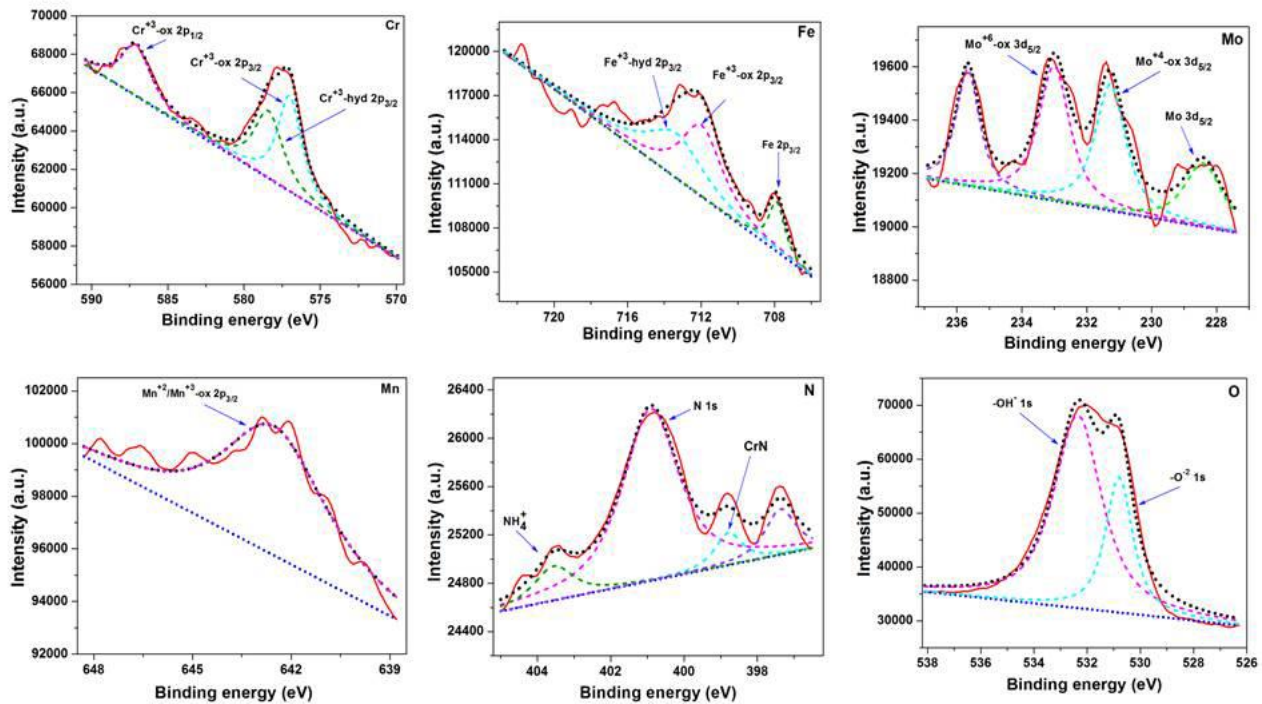
Fig.3(i): The X-ray photoelectron spectra recorded from the passive film of annealed stainless steels (316LMnN$_3$)

The O 1s peak resolved into oxide (ox) and hydroxide (hy) at binding energy value of about 530.4 eV and 532.0 eV respectively. Fe 2p$_{3/2}$ peak resolved into its oxide, and hydroxide forms with binding energy of about 711.5 and 713.0 eV respectively

9

and Cr $2p_{3/2}$ peak also resolved to oxide and hydroxide forms with binding energy of about 577.0 and 578.3 eV respectively. The film of Cr and Fe is made up of two layers- -oxide and a hydroxide. A bilayer passive film composed of oxide and hydroxide has also been proposed by Raja et al. [20] Elemental peak was not detected for Cr but for Fe at binding energy 707.8 eV.
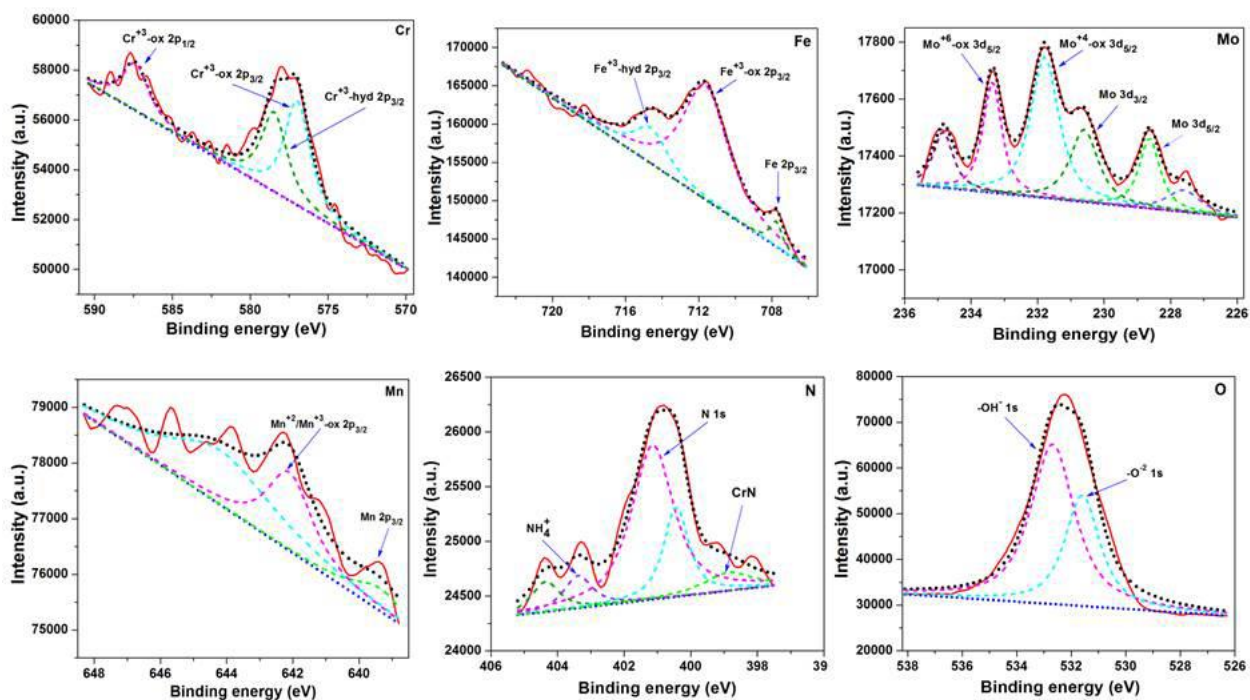
Fig.3(ii): The X-ray photoelectron spectra recorded from the passive film of 20 % cold worked stainless steels (316LMnN$_3$)

The absence of nickel in the film agrees with the work of Halada et al.[21] and S.V. Phadnis et al.[22] on SSs. Study by Chen et al.[23] on SS 304 has shown the film to contain about 2-3% nickel. The films analyzed here showed no nickel peak for

annealed as well as 20% cold worked samples. It is assumed that nickel is preferably leached out of the film [24] or it gets enriched in the substrate [21]. Phadnis et al.[22] have reported that nickel does not leach out of the film but chromium and iron diffuse out preferentially to form the passive film due to their high oxygen affinity while nickel gets enriched in the substrate. Mo^{+4} and Mo^{+6} oxide peaks were obtained for all the samples along with elemental peaks. One additional elemental peak of Mo 3d $_{3/2}$ was also obtained for 20% cold worked samples, indicating slightly more percentage of Mo on cold worked surface. The Cr–N peak was also detected for $316MnN_3$ at binding energy 398.8 eV. The oxide peaks are stronger for the 20% cold worked specimen in comparison with annealed one as shown in Table 3. The protection of the passive film in annealed specimen is weaker might be due to the presence of more hydroxides, which can lead to impairment of the resistance to localized corrosion.[25] Similar results were also obtained in our previous study for nickel containing stainless steels in SBF [26]. The more stable passive film, thus increases film resistance resulted in improved corrosion resistance for cold worked samples in Ringer's solution.

Table 3

Ratio of oxide and hydroxide of Cr and Fe on surface of stainless steels obtained by XPS analysis.

Sample	Condition	$I_{Cr\text{-}ox}/I_{Cr\text{-}hy}$	$I_{Fe\text{-}ox}/I_{Fe\text{-}hy}$
$316MnN_3$	annealed	1.09	1.40
	20% c.w.	1.38	1.92

3.3. X-ray diffraction (XRD) analysis

Fig. 4 shows the X-ray diffraction profiles of annealed as well as deformed alloys with 20% thickness reduction at room temperature. XRD investigations exposed only the presence of phases corresponding to austenite with γ (111) and γ (220) as the preferred planes and no evidences for formation of martensite or any other secondary phase.
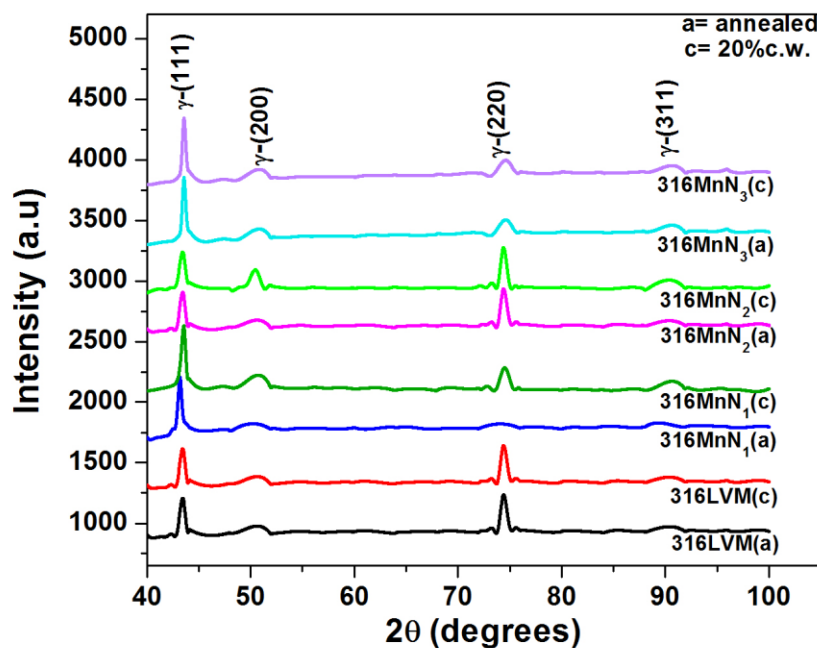
Fig. 4: XRD patterns of annealed and cold rolled SS samples.

It was suggested that in nitrogen containing steels at the top layers of the passive alloying elements would have converted into their oxide and simultaneously dissolved the alloying elements into the solution, leaving the nitrogen at the surface. At one stage, dissolution of these alloying elements became slow due to the increase in the concentration of nitrogen at the surface, hindering the further attack of the aggressive chloride ions. It resulted in the enrichment of nitrogen and depletion of oxygen observed at the surface. The enrichment of nitrogen at the surface inhibited the oxide species from approaching the metal constituent for further oxide growth [27]. It was also suggested that the interface enrichment of nitrogen could act as a protecting layer from penetration of the harmful ions [28]. In this study the weight loss of $316MnN_1$, which contains carbon, is less than 316LVM, indicating that carbon has no effect on the protective layers on surface of SSs. Rolling results in a preferential texture of high

13

index low density planes along the rolling direction of austenitic SSs. The effect of this texture resulting in a reduced binding energy of atoms in this less close packed plane can result in enhanced dissolution in acidic chloride medium, where metal dissolution step plays a predominant role in the rate control mechanism. This is not in the case of neutral chloride solution, where oxygen diffusion was the rate-controlling step. The reason for the above difference might be partially due to differences in the materials and solution systems considered. Moreover, it was also detected that the chromium content in passive film formed on deformed austenitic SS surface was richer than that formed on heat treated samples, and the higher chromium content improved corrosion resistance of passive films [22]. In the case of the heat treated alloy the film being thinner and with less Cr:Fe ratio, it is less protective as compared with the rolled alloy [22, 26]. Hamdy et al. [13] revealed that the surface of 23% cold deformed austenitic SS had a smooth appearance and uniform distribution of surface oxide layer. The presence of uniformly distributed surface oxide layer decreases the surface defects due to which active anodic sites decreases which is the main source for the occurrence of localized corrosion.

4. Conclusions

From the present investigation the following conclusions can be made:

- Nitrogen content and prior cold work showed a significant influence on the corrosion behavior of SSs. The weight loss and corrosion rates decreased with increasing nitrogen content in the alloy and degree of cold work.

14

- The XPS results showed that the main elements of the oxide layer on steels are Cr, Fe and Mo. Cr-ox:Cr-hy ratio and Fe-ox:Fe-hy ratio were observed higher in case of rolled material than annealed material indicating that the passive films on rolled materials are more stable and protective which improve its corrosion resistance.
- XRD investigations revealed that there is no evidence for formation of martensite or any other secondary phases up to 20% cold working.

References

[1] S. Nagarajan, N. Rajendran, Surface characterisation and electrochemical behaviour of porous titanium dioxide coated 316L stainless steel for orthopaedic applications, Appl. Surf. Sci., 2009, **255**, 3927-3932.

[2] A. Yamamoto, D. Kohyama, D. Kuroda, T. Hanawa, Cytocompatibility evaluation of Ni-free stainless steel manufactured by nitrogen adsorption treatment, Materials Science and Engineering C, 2004, **24**, 737-743.

[3] C. Schmidt, Ignatius A, Claes LE, Proliferation and differentiation parameters of human osteoblasts on titanium and steel surfaces, J. Biomed. Mater. Res., 2001, **54**, 209-215.

[4] I. Kimber, D.A. Basketter, Contact Hypersensitivity to Metals in: Chang LW (Ed.), Toxicology of Metals, CRC Press, Boca Raton, 827-834, 1996.

[5] IARC Monographs on the Evaluation of Carcinogenic Risks to Humans: Surgical Implants and Other Foreign Bodies, Lyon, vol. 74, p. 65, 1999.

[6] M. Talha, C.K. Behera, O.P. Sinha, In-vitro long term and electrochemical corrosion resistance of cold deformed nitrogen containing austenitic stainless steels in simulated body fluid, Materials Science and Engineering C, 2014, **40**, 455-466.

[7] J. Menzel, W. Kirschner, G. Stein, High Nitrogen Containing Ni-free Austenitic Steels for Medical Applications, ISIJ Int., 1996, **36**, 893-900.

[8] M. Talha, C.K. Behera, O.P. Sinha, A review on nickel-free nitrogen containing austenitic stainless steels for biomedical applications, Materials Science and Engineering C, 2013, **33**, 3563-3575.

[9] Z. Szklarska-Smialowska, Review of literature on pitting corrosion published since 1960, Corrosion, 1971, **27**, 223-233.

[10]   A.J. Sedriks, in: Proceedings of the International Conference on Stainless Steels 85, The Institute of Metals, London, p. 125, 1985.

[11]   U.K. Mudali, P. Shankar, S. Ningshen, R.K. Dayal, H.S. Khatak, Baldev Raj, On the pitting corrosion resistance of nitrogen alloyed cold worked austenitic stainless steels, Corrosion Science, 2002, **44**, 2183-2198.

[12]   L. Peguet, B. Malki, B. Baroux, Influence of cold working on the pitting corrosion resistance of stainless steels, Corrosion Science, 2007, **49**, 1933-1948.

[13]   A.S. Hamdy, E. El-Shenawy, T. El-Bitar , The corrosion behavior of niobium bearing cold deformed austenitic stainless steels in 3.5% NaCl solution, Materials Letters, 2007, **61**, 2827-2832.

[14]   J. Beddoes, K. Bucci, The influence of surface condition on the localized corrosion of 316L stainless steel orthopaedic implants, J. Mater. Sci. Mater. Med., 1999, **10**, 389-394.

[15]   S. Karimi, T. Nickchi, A.M. Alfantazi, Long-term corrosion investigation of AISI 316L, Co-28Cr-6Mo, and Ti-6Al-4V alloys in simulated body solutions, Applied Surface Science, 2012, **258**, p.6087-6096.

[16]   ASTM Standard D5245, 2005, Standard Practice for Cleaning Laboratory Glassware, Plasticware, and Equipment used in Microbiological analyses, ASTM, International, West Conshohocken, PA, 1992, doi:10.1520/D5245-92R05, www.astm.org

[17]   M. Talha, C.K. Behera, O.P. Sinha, Potentiodynamic polarization study of Type 316L and 316LVM stainless steels for surgical implants in simulated body fluids, J. of Chemical and Pharmaceutical Research, 2012, **4**, 203-208.

[18]   H. Yang, K. Yang, B. Zhang, Pitting corrosion resistance of La added 316L stainless steel in simulated body fluids, Materials Letters, 2007, **61**, 1154-1157.

[19]   ASTM Standard G31, 2004, Standard Practice for Laboratory Immersion Corrosion Testing of Metals, ASTM, International, West Conshohocken, PA, 1972, doi:10.1520/G0031-72R04, www.astm.org.

[20]   V.S. Raja, P. Veluchamy, H. Minoura, Electron Spectroscopy for Chemical Analysis Study of Corrosion Films Formed on Manganese Stainless Steels, Corrosion, 1999, 55, 1119-1126..

[21]   G.P. Halada, D. Kim, C.R. Clayton, Influence of Nitrogen on Electrochemical Passivation of High-Nickel Stainless Steels and Thin Molybdenum-Nickel Films, Corrosion, 1996, 52, 36-46.

[22]   S.V. Phadnis, A.K. Satpati, K.P. Muthe, J.C. Vyas, R.I. Sudaresan, Comparison of rolled and heat treated SS304 in chloride solution using electrochemical and XPS techniques, Corrosion Science, 2003, 45, 2467-2483.

[23]   G. Chen, S.V. Kagwade, G.E. French, T.E. Ford, R. Mitchel, C.R. Clayton, Metal ion and expolymer interaction: A surface analytical study, Corrosion, 1996, 52, 891-899.

[24]   S. Jin, A. Atrens, ESCA studies of the surface film formed on stainless steels by exposure to 0.1M NaCl solution at various controlled potentials, Appl. Phys. A, 1988, 46, 51-65.

[25]   C.R. Clayton, Y.C. Lu, A bipolar model of the passivity of stainless steel: The role of molybdenum addition, J. Electrochem. Soc., 1986, 133, 2465-2473

[26]   M. Talha, C.K. Behera, S. Kumar, O. Pal, G. Singh, O.P. Sinha, Long term and electrochemical corrosion investigation of cold worked AISI 316L and 316LVM stainless steels in simulated body fluid RSC Adv., 2014, 4, 13340-13349.

[27]　　T. Sundararajan, U.K. Mudali, K.G.M. Nair, S. Rajeswari, M. Subbaiyan, Effect of nitrogen ion implantation on the localized corrosion behavior of titanium modified type 316L stainless steel in simulated body fluid, Journal of Materials Engineering and Performance, 1999, **8**, 252–260.

[28]　　Y. Fu, X.Q. Wu, E.H. Han, W. Ke, K.Yang, Z. Jiang, Effects of nitrogen on the passivation of nickel–free high nitrogen and manganese stainless steels in acidic chloride solutions, Electrochim. Acta, 2009, **54**, 4005–4014.